Three-dimensional MRI-linac intra-fraction guidance using multiple orthogonal cine-MRI planes

Troels Bjerre[1,2], Sjoerd Crijns[3], Per Munck af Rosenschöld[2], Marianne Aznar[2], Lena Specht[4], Rasmus Larsen[1] and Paul Keall[5]

[1] Department of Applied Mathematics and Computer Science, Technical University of Denmark, Denmark

[2] Radiation Medicine Research Center, Department of Radiation Oncology, Niels Bohr Institute, University of Copenhagen, Denmark

[3] Department of Radiotherapy, University Medical Center Utrecht, Netherlands

[4] Department of Oncology, Rigshospitalet, University of Copenhagen, Denmark

[5] Radiation Physics Laboratory, University of Sydney, Australia

Corresponding Author : Troels Bjerre trbj@dtu.dk

Abstract

The introduction of integrated MRI-radiation therapy systems will offer live intra-fraction imaging. We propose a feasible low-latency multi-plane MRI-linac guidance strategy. In this work we demonstrate how interleaved acquired, orthogonal cine-MRI planes can be used for low-latency tracking of the 3D trajectory of a soft-tissue target structure. The proposed strategy relies on acquiring a pre-treatment 3D breath-hold scan, extracting a 3D target template and performing template matching between this 3D template and pairs of orthogonal 2D cine-MRI planes intersecting the target motion path. For a 60 s free-breathing series of orthogonal cine-MRI planes, we demonstrate that the method was capable of accurately tracking the respiration related 3D motion of the left kidney. Quantitative evaluation of the method using a dataset designed for this purpose revealed a translational error of 1.15 mm for a translation of 39.9 mm. We have demonstrated how interleaved acquired, orthogonal cine-MRI planes can be used for online tracking of soft-tissue target volumes.

1. Introduction

Integrated MRI-radiotherapy systems are currently under development, as described by Lagendijk *et al* (2008), Raaymakers *et al* (2009), Fallone *et al* (2009), Dempsey and 'VIEWRAY Inc.' (2011), Dempsey *et al* (2005). While not widely available, such systems offer live intra-fraction imaging, thus facilitating non-invasive, non-surrogate based, low-latency tumor motion tracking with no additional imaging radiation dose. Online tracking of target volumes in image-guided radiotherapy has great potential to increase conformality when treating tumors affected by respiratory motion. Tumor dose is thereby maximized while the dose to surrounding healthy tissue is minimized (Verellen *et al* 2007). This enables dose escalation, providing for a higher tumor control probability.

The AAPM Task Group 76 report by Keall *et al* (2006) concluded that lung tumors can follow

complex 3D trajectories. An intra-fraction tracking method should therefore preferably provide 3D coordinates of the tumor. Possible breathing irregularities necessitates that the latency of an online tracking system be kept as low as possible. Keall *et al* (2006) suggests that an upper latency limit for an online tracking system should be 0.5 s. Ries *et al* (2010) shows that an MRI tracking system with a 10 Hz imaging rate, 100 ms processing latency and a Kalman predictor provides a 0.9 mm tracking error for tracking the motion of a kidney. Such tracking error will be close to the voxel size delivered by most MRI systems.

Acquisition of high-quality live 3D images with subsequent low-latency deformable image registration (DIR) would be optimal, but is currently not feasible due to the lack of appropriate MRI acquisition sequences and DIR algorithms.

Previous efforts have focused on tracking in 2D cine-MRI planes. Cerviño *et al* (2011) suggested the use of template matching for real-time lung tumor tracking in sagittal cine-MRI scans. An inherent drawback of tracking a 3D structure in a 2D plane is the inability to detect out-of-plane motion. They suggest addressing out-of-plane motion by surrogate tracking of the diaphragm. Yun *et al* (2012b) investigated the use of an intra-fractional lung tumor auto- contouring algorithm for a phantom study using sagittal cine-MRI planes. Yun *et al* (2012a) describes how the auto-contouring algorithm of Yun *et al* (2012b) can be extended with an artificial neural network-based motion prediction algorithm.

Ries *et al* (2010) performed 3D target tracking by combining 2D-plane imaging with prospective slice tracking based on pencil-beam navigator sequences. The effect of the update latency was reduced using a Kalman predictor for trajectory anticipation. One limitation they find is that since the detected beam signal is predominantly spin-density weighted, it suffers from poor tissue contrast, which can potentially lead to poor tracking performance.

We have developed and investigated a 3D tracking strategy feasible for low-latency, intrafraction magnetic resonance imaging-linear accelerator (MRI-linac) guidance. The proposed strategy is based on template matching between a 3D target template obtained from a pretreatment breath-hold MRI scan and sets of orthogonal cine-MRI planes. We use interleaved acquired coronal and sagittal cine-MRI scan planes, intersecting the motion path of the tracked structure in the subject.

We seek to illustrate that the method facilitates 3D motion tracking, that the use of orthogonal planes is superior to tracking 2D target templates on a single cine-MRI plane, and that the method is feasible for online tracking of soft-tissue target volumes.

2. Methods

The clinical scenario under which this method would operate involves the acquisition of a pre-treatment breath-hold 3D MRI scan from which a 3D template containing the target is extracted.

The similarity between the 3D template and pairs of cine-MRI 2D coronal and sagittal planes is calculated for each combination of investigated (posterior–anterior (PA), right–left (RL), inferior–superior (IS)) translations of the 3D template. If the resolution of the 3D template differs from the resolution of the 2D planes, interpolation is required.

The 3D bounding box, V_C, with dimensions N_{PA} x N_{RL} x N_{IS} encompasses the entire irregularly shaped target volume V_T .

The 3D target template can be thought of as a set of 2D coronal target slices as well as a set of sagittal target slices encompassing the segmented target

$$S_{cor} = \{s_{cor,1},..,s_{cor,N_{PA}}\}, \quad (1)$$

$$S_{sag} = \{s_{sag,1},..,s_{sag,N_{RL}}\}, \quad (2)$$

where each slice spans the target volume in that particular orientation and plane, e.g.

$$s_{cor,1} = V_C(1, i_{RL}, i_{IS}) \quad (3)$$

$$i_{RL} = [\min_{RL} - b, \ldots, \max_{RL} + b] \quad (4)$$

$$i_{IS} = [\min_{IS} - b, \ldots, \max_{IS} + b)], \quad (5)$$

where $\min_{RL}$, $\max_{RL}$, $\min_{IS}$, $\max_{IS}$ are the minimum and maximum voxel indices of segmented target volume voxels in that particular slice. This means that the set of target slices in one orientation are not necessarily of the same dimension. Here, b is an additional border that can be added to improve tracking robustness if necessary. On the other hand, adding too wide a border might deteriorate accuracy.

For each set of interleaved acquired coronal and sagittal 2D cine-MRI planes, P_{cor}, P_{sag}, a similarity measure is evaluated between P_{cor} and the individual slices of the coronal target slice set S_{cor} and between P_{sag} and the slices of S_{sag}. The similarity measure is evaluated for all investigated combinations of PA, RL and IS translations of the target template, with T_{PA}, T_{RL}, T_{IS} being the total number of investigated translations in each direction. This results in T_{PA} 2D coronal similarity arrays d_{cor} of size T_{RL} x T_{IS} and T_{RL} 2D sagittal similarity arrays d_{sag} of size T_{PA} x T_{IS}. The arrays are normalized by subtracting each array by the lowest of the array itself.

The coronal and sagittal 2D similarity arrays are coalesced into two 3D similarity arrays, D_{cor}, D_{sag} both of size T_{PA} x T_{RL} x T_{IS}. Subsequently, the combined similarity array, D_{total}, is determined by adding the normalized coronal and sagittal similarity arrays,

$$D_{total} = D_{cor,normalized} + D_{sag,normalized}. \quad (6)$$

The optimal translation is the one with the highest combined similarity measure,

$$\max(D_{total}) \rightarrow t_{optimal}. \quad (7)$$

t

The normalization is performed in order for the similarity values of the coronal and sagittal array to be approximately on the same scale. If not normalized, one array might dominate D_{total}. If the

orthogonal slices have different resolutions, further normalization might be needed.

As similarity measure for the template matching we applied mean-absolute-difference (MAD). Other methods, including mean-squared-error (MSE) and normalized cross-correlation were considered, but generally gave inferior results for the data at hand. Note that MAD and MSE are actually dissimilarity measures for which equation (6) is minimized in order to maximize similarity.

Breath-hold scans and cine-MRI scans were acquired using the same sequence so that normalization was not required. In order to apply traditional template matching algorithms, the template was interpolated to the same pixel size as the orthogonal planes.

A basic assumption for this method is local rigidity of the target volume. The method should be suitable for target sites where this approximately holds. We acquired coronal and sagittal planes, but all directions could be used, as long as the tracked structure is intersected by the orthogonal planes at all times. If the target volume is too small to ensure this, additional border can be added to the target template as described above.

2.1. Qualitative evaluation

For a qualitative evaluation of the method, we acquired a 3D exhale MRI scan and a series of interleaved acquired orthogonal cine-MRI planes. We segmented the 3D target structure from the exhale scan by manual delineation, and then performed tracking on all pairs of cine planes in a one-minute sequence, thus estimating the position of the target center in 3D. Since the true position of the target volume center in 3D cannot be known during this type of acquisition, the result is evaluated using visual inspection, by superimposing the target volume delineation on the cine-MRI scans according to the estimated translation of the volume.

The true position can only be known for acquisition of 3D volumes with no motion, i.e. during breath-hold or using very fast sequences with inherently poor signal-to-noise ratio.

2.2. Quantitative evaluation

In order to quantify the accuracy of the method, we acquired 3D inhale and exhale breath-hold MRI scans and segmented the target structure in both breathing phases by manual delineation. This gives us the true difference in position of the target structure in these two breath-hold states. We then compared the true difference in location of the center of the target volume to the one approximated using tracking of the 3D target template from the exhale scan on a sagittal and coronal slice pair, extracted from the 3D inhale breath-hold scan. This approach simulates tracking on cine-MRI planes while knowing the actual true position of the target center of volume.

The true difference in location of the target center of volume is established by delineating the 3D target volume in the 3D inhale and exhale scans, calculating the center of the target volume and calculating the PA, RL and IS differences in location.

We compared our multi-plane 3D tracking method to 2D tracking as demonstrated by Cerviño *et al* (2011). This was done by using the segmented target on one sagittal or coronal slice in the exhale scan as template and tracking this template in the same coronal or sagittal slice plane of the inhale scan.

2.3. Data for qualitative evaluation

This method is applicable to all tumor sites affected by respiratory motion. We tested the method in a healthy subject, tracking the left kidney during respiration.

All data was acquired on a 1.5 T Philips Achieva system using an eight channel torso receive coil.

The orthogonal cine-MRI planes were interleaved acquired during free breathing using a balanced steady-state free precession (bSSFP) sequence with the following parameters TR/TE 2.7/1.34 ms, FOV 40 x 40 cm^2, flip angle = 35°, slice thickness = 7 mm, in-plane voxel size =1.05 mm, parallel imaging factor 2, acquisition time per plane = 0.252 s.

At the intersection between the orthogonal planes, less signal is received which results in a dark line. This is compensated for prior to the template matching, by multiplying each line of the cine-MRI plane by 1 + 0.4* *G*, where $G = \exp(-0.5\frac{x-c}{w})$ is a (non-normalized) 1D Gaussian kernel with a kernel width of 3 pixel widths and center *c* at the intersection between the orthogonal planes. The optimal kernel width has been chosen by visual inspection. This is an ad hoc empirical solution.

A 3D exhale breath-hold scan was acquired using a bSSFP sequence similar to the one used for the cine-MRI planes using the following parameters TR/TE = 2.7/1.34 ms, FOV = 12 x 31 x 31 cm^3 (PA, LR, IS), flip angle = 35°, slice thickness = 2 mm, in-plane voxel size = 1.1 mm, acquisition time = 25 s.

The target structure, the left kidney, was manually contoured using the Varian Eclipse software (Varian Medical Systems Inc.). For a clinical implementation, target auto-segmentation could be employed. Using MATLAB for further pre-processing, the 3D scan was interpolated to the same resolution as the orthogonal cine-MRI planes, and filtered with a Gaussian kernel for improving tracking robustness. By applying this low pass filtering operation we sought to ensure that the algorithm reach a global similarity maximum and not a local one by enhancing the dominant features of the template.

2.4. Data for quantitative evaluation

3D exhale and inhale breath-hold scans were acquired using the same 3D sequence as for the qualitative evaluation data. The target structure, the left kidney, was manually contoured in both scans and pre-processed in the same manner as the scan for qualitative evaluation.

3. Results

3.1. Qualitative evaluation

Figure 1 displays the measured translation of the left kidney during a one-minute interleaved acquisition sequence of coronal and sagittal cine-MRI planes. The initial use of no additional voxel border on the sets of target slices resulted in a few deviations (discontinuities of center of volume trajectory). By using a border width of three voxels these few deviations were avoided due to added robustness. By visual inspection, tracking accuracy on the remaining frames did not seem deteriorated by the use of the border. Correlation between the time-series of IS and PA translation was -0.83. Correlation between IS and RL translation was 0.83. The maximum peak-to-peak translations in *(*PA, LR, IS*)* directions were *(*4.2, 3.2, 16*)* mm, respectively. The standard deviation of target position in (PA, LR, IS) directions were *(*0.70, 0.75, 3.8*)* mm, respectively

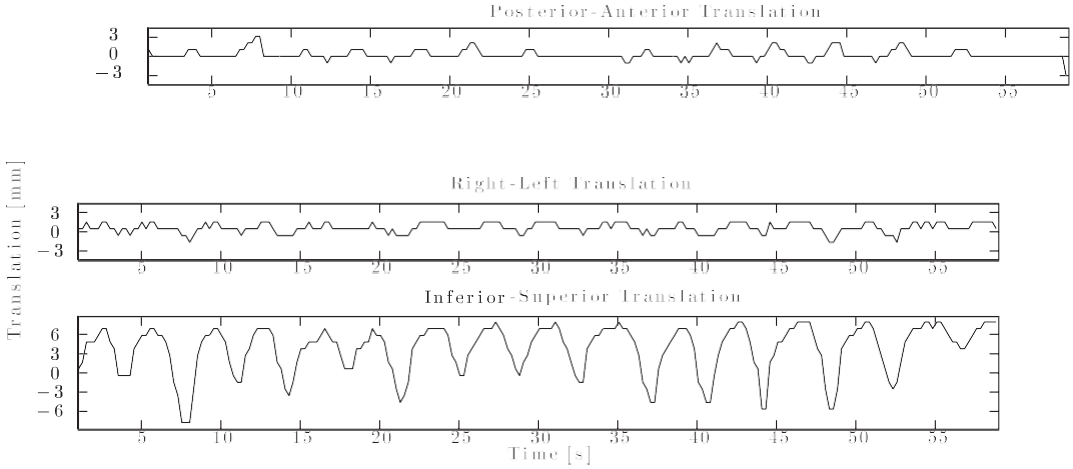

Figure 1. This figure displays posterior–anterior (PA), right–left (RL) and inferior–superior (IS) translation of the left kidney as a function of time during free breathing. In the plot of IS position the peaks represent exhalation while the troughs represent inhalation. The translation was determined using the multi-plane guidance method for pairs of interleaved acquired coronal and sagittal cine-MRI planes. Acquisition frequency was 4 Hz.

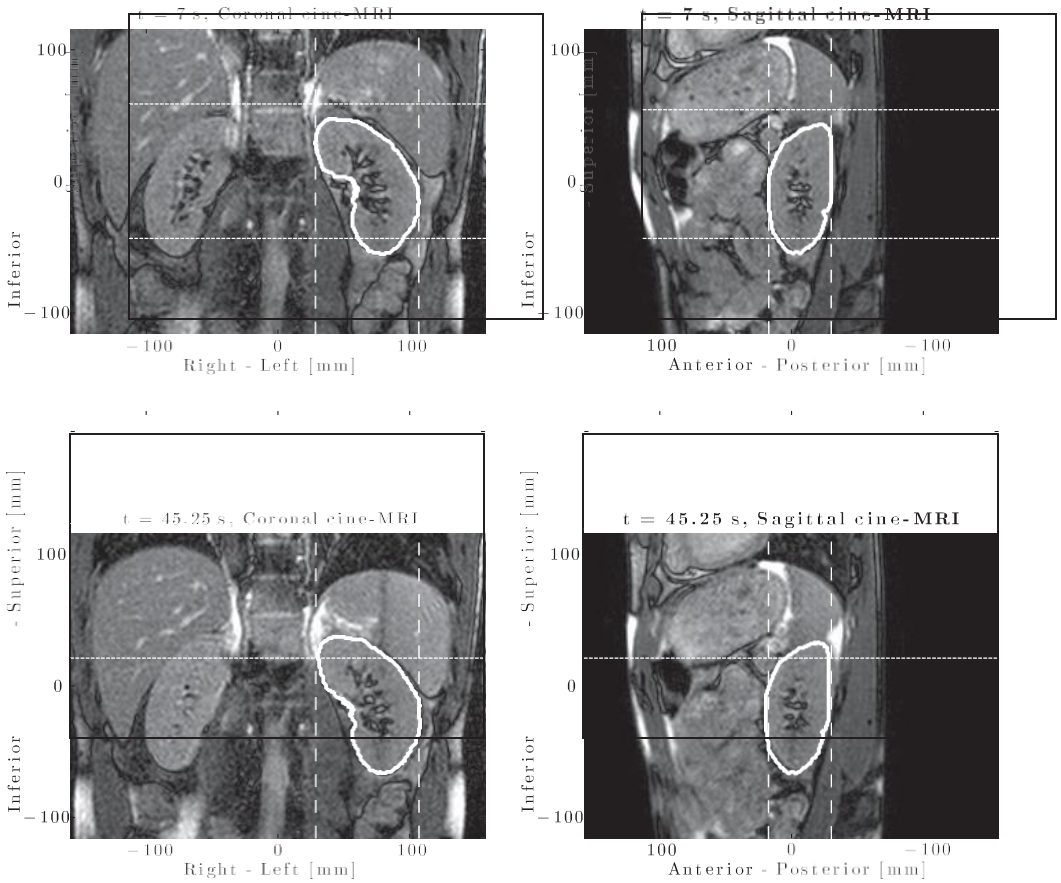

Figure 2. For two points in time during free breathing, *t= (*7, 45.25*)* s, this figure displays pairs of interleaved acquired coronal and sagittal cine-MRI planes. The 3D kidney delineation from the exhale breath-hold scan is superimposed on the cine-MRI planes (solid white), according to translation determined using our multi-plane 3D tracking method. The dotted white lines are at the same positions in the scans and are included only to emphasize the soft-tissue motion between the time points.

Figure 2 displays two pairs of coronal and sagittal cine-MRI planes from the sequence. The 3D kidney delineation from the exhale breath-hold scan is superimposed on the cine-MRI planes, according to the translation providing maximum similarity, using our multi-plane 3D tracking method.

See supplementary material for a video that shows all orthogonal cine-MRI pairs of the acquired one-minute sequence with superimposed delineation.

The mean processing time for a slice pair was 153 ms for a 53 x 83 x 111 voxel template with a non-parallelized MATLAB implementation on an Intel I7–620 M processor.

3.2. Quantitative evaluation

Table 1 presents the results of the quantitative evaluation. The table compares the difference in accuracy between 3D tracking on orthogonal cine-MRI planes and 2D tracking on a single sagittal or coronal plane.

The use of different border widths around the delineated area in the slices of the 3D template was investigated. The use of no border gave the most accurate result.

Table 1. This table compares the true difference in location of the center of volume of the left kidney between 3D inhale and exhale breath-hold MRI scans with the approximated difference in location. The difference is approximated using 3D tracking of the 3D kidney template from the exhale scan on a sagittal and coronal slice pair from the inhale scan, emulating cine-MRI planes (denoted by S+C) as well as by using 2D tracking of single sagittal or coronal slice kidney templates from the exhale scan tracked on the same sagittal or coronal slice of the inhale scan (denoted S and C, respectively). The calculated error is the Euclidean difference between the true and estimated position.

		Appr.difference (mm)			Error (mm)		
True difference in location (mm)		S	C	S + C	S	C	S + C
Posterior-anterior	10.5	9.38	0	9.38	1.09	10.5	1.09
Right-left	−3.46	0	−6.25	−3.13	−3.46	2.79	−0.34
Inferior-superior	−38.3	−38.5	−38.5	−38.5	0.2	0.2	0.2
Total (Euclidean)	39.9	39.7	39.0	39.8	3.63	10.8	1.15

4. Discussion and conclusions

We have developed a low-latency MRI-linac guidance strategy, feasible for intra-fraction image-guidance during radiotherapy. Obtaining low-latency information about the 3D target trajectory is the single most important feature of our multi-plane tracking method.

Intra-fraction image guidance allows for improved conformality and maximization of the therapeutic ratio by increasing dose to target tissues and decreasing dose to healthy tissue. We have shown that by using orthogonal, interleaved acquired cine-MRI planes it is possible to track the 3D trajectory of a soft-tissue target structure. From visual inspection, tracking of the kidney in the one-minute cine-MRI sequence appears very accurate and robust.

It is interesting but not surprising that there was a relatively large correlation between motion in the three dimensions. However, based on the translations in figure 1, it is not possibly to predict the PA and LR translations from the IS translation alone.

The quantitative evaluation results indicate errors of total 3D motion on the scale of the width of a cine-MRI pixel (1.04 mm). The use of orthogonal planes was superior to using only a sagittal or coronal plane. Investigations using 3D breath-hold scans at different inhalation states or 4D MRI could be used to further validate these results. This is merely the overall translational error, assuming local rigidity, and does not reflect on any delineation uncertainty or deformation between the phases, nor the uncertainty related to the breath-hold acquisition. It is noteworthy that any number

and orientation of intersecting live planes could be used,

as long as the target is intersected by the planes at all times. Further investigation on a variety of patient cases and target sizes/locations will be needed to more broadly characterize the performance of this guidance strategy.

The use of two orthogonal cine-MRI planes inherently increases the time between two successive scans of the same plane. In cases with linear trajectory of the target volume it would be possible to avoid the out-of-plane motion when using a single cine-MRI plane by choosing an appropriate orientation. In these cases, using a single cine-MRI plane could be superior to using the proposed multi-plane method due to the higher temporal resolution.

The processing time for the current implementation allows the total system delay to be below the 0.5 s prescribed by Keall *et al* (2006), thus allowing the method to be fast enough for online tracking. It should be straightforward to implement parallel processing for a further reduction of processing time. Parallel processing could also facilitate rotation-invariant template matching by processing 3D templates with different rotation. For further robustness, and in order to prevent any eventual deviations, the described method could be extended with a prediction algorithm. The adoption of a scale-space strategy might be appropriate for improving tracking robustness and further reduce processing time, see e.g. Witkin (1984).

While this work focuses on MRI-linac guidance, the described method is relevant for other applications as well, including MRI high-intensity focused ultrasound systems.

References

Cerviño L I, Du J and Jiang S B 2011 MRI-guided tumor tracking in lung cancer radiotherapy *Phys. Med. Biol.* **56** 3773–85

Dempsey J, Benoit D, Fitzsimmons J, Haghighat A, Li J, Low D, Mutic S, Palta J, Romeijn H and Sjoden G 2005 A device for realtime 3D image-guided IMRT *Int. J. Radiat. Oncol. Biol. Phys.* **63** 202

Dempsey J and VIEWRAY Inc.' 2011 System and method for image guidance during medical procedures *US Patent Specifications* WO/2012/088321

Fallone B G, Murray B, Rathee S, Stanescu T, Steciw S, Vidakovic S, Blosser E and Tymofichuk D 2009 First MR images obtained during megavoltage photon irradiation from a prototype integrated linac-MR system *Med. Phys.* **36** 2084

Keall P J *et al* 2006 The management of respiratory motion in radiation oncology report of AAPM Task Group 76 *Med. Phys.* **33** 3874

Lagendijk J J W, Raaymakers B W, Raaijmakers A J E, Overweg J, Brown K J, Kerkhof E M, van der Put R W, Hårdemark B, van Vulpen M and van der Heide U A 2008 MRI/linac integration *Radiother. Oncol.* **86** 25–29

Raaymakers B W *et al* 2009 Integrating a 1.5 T MRI scanner with a 6 MV accelerator: proof of concept *Phys. Med. Biol.* **54** N229–37

Ries M, de Senneville B D, Roujol S, Berber Y, Quesson B and Moonen C 2010 Real-time 3D target tracking in MRI guided focused ultrasound ablations in moving tissues *Magn. Reson. Med.* **64** 1704–12

Verellen D, De Ridder M, Linthout N, Tournel K, Soete G and Storme G 2007 Innovations in

image-guided radiotherapy *Nature Rev. Cancer* **7** 949–60

Witkin A P 1984 Scale-space filtering: a new approach to multi-scale description *IEEE Trans. Acoust. Speech Signal Process.* **9** 150–3

Yun J, Mackenzie M, Rathee S, Robinson D and Fallone B G 2012a An artificial neural network (ANN)-based lung-tumor motion predictor for intrafractional MR tumor tracking *Med. Phys.* **39** 4423–33

Yun J, Yip E, Wachowicz K, Rathee S, Mackenzie M, Robinson D and Fallone B G 2012b Evaluation of a lung tumor autocontouring algorithm for intrafractional tumor tracking using low-field MRI: a phantom study *Med. Phys.* **39** 1481–94.